Quantum Monte Carlo Simulations of the 2D Su-Schrieffer-Heeger Model

Bo Xing, Wei-Ting Chiu, Dario Poletti, R. T. Scalettar, and George Batrouni

Phys. Rev. Lett. **126**, 017601 — Published 7 January 2021

DOI: 10.1103/PhysRevLett.126.017601

Quantum Monte Carlo Simulations of the 2D Su-Schrieffer-Heeger Model

Bo Xing,[1] Wei-Ting Chiu,[2] Dario Poletti,[1,3] R.T. Scalettar,[2] and George Batrouni[4,5,6,7]

[1]*Science, Mathematics and Technology Cluster, Singapore University of Technology and Design, 8 Somapah Road, 487372 Singapore*
[2]*Department of Physics, University of California, Davis, CA 95616, USA*
[3]*Engineering Product Development Pillar, Singapore University of Technology and Design, 8 Somapah Road, 487372 Singapore*
[4]*Université Côte d'Azur, INPHYNI, CNRS, 0600 Nice, France*
[5]*Centre for Quantum Technologies, National University of Singapore, 2 Science Drive 3, 117542 Singapore*
[6]*Department of Physics, National University of Singapore, 2 Science Drive 3, 117542 Singapore*
[7]*Beijing Computational Science Research Center, Beijing, 100193, China*

(Dated: November 30, 2020)

Over the last several years, a new generation of quantum simulations has greatly expanded our understanding of charge density wave phase transitions in Hamiltonians with coupling between local phonon modes and the on-site charge density. A quite different, and interesting, case is one in which the phonons live on the bonds, and hence modulate the electron hopping. This situation, described by the Su-Schrieffer-Heeger (SSH) Hamiltonian, has so far only been studied with quantum Monte Carlo in one dimension. Here we present results for the 2D SSH model, and show that a bond ordered wave (BOW) insulator is present in the ground state at half-filling, and argue that a critical value of the electron-phonon coupling is required for its onset, in contradistinction with the 1D case where BOW exists for any nonzero coupling. We determine the precise nature of the bond ordering pattern, which has hitherto been controversial, and the critical transition temperature, which is associated with a spontaneous breaking of $\mathcal{Z}_4$ symmetry.

Introduction: The Su-Schrieffer-Heeger (SSH) model [1], where lattice vibrations (phonons) modulate the ability of electrons to tunnel between neighboring sites (*i.e.* the hopping parameter), was proposed more than four decades ago to describe the Peierls-wave, bond ordered wave (BOW), phase transition from a metal to an insulator, driven by the lowering of the electronic kinetic energy. The SSH model considered this transition in the context of polyacetylene, but the instability has long been known to occur experimentally in other quasi-1D systems, including conjugated polymers [2], organic charge transfer salts [3], MX salts [4], and $CuGeO_3$ [5].

Furthermore, the SSH paper [1] already recognized the possibility of topological excitations with fractional charge. Over the last decade, tunable cold atom systems have achieved real space superlattices [6, 7], enabling the emulation of the SSH Hamiltonian [8–10] as a simple realization of 1D "BDI" class topological insulators [11, 12] (*i.e.* possessing spin rotation, time reversal, and particle hole symmetries). Understanding the underlying ordered phases and phase transitions in two dimensions (thermal and quantum), as presented here, lays the foundation towards studying the competition between electron-phonon and electron-electron interactions and the possible existence of topological phases.

Early numerical work on the 1D SSH model addressed whether the bond (Peierls) distortion survives fluctuations in the phonon field, and indicated [13] differences between the spinless and spinful SSH models, where the latter was argued to be always ordered (albeit with a reduced order parameter as the phonon frequency increases), and the former to have order-disorder transitions [14–16]. Subsequent numerical and renormalization group studies [17–21] confirmed that lattice fluctuations do not induce metallic behavior for spinful fermions. Analogous questions have been addressed in the Holstein model [13, 19, 22–25]. Polaron and bipolaron formation, along with condensation into superfluid states, have also been areas of considerable activity [21, 26, 27].

These interesting and challenging 1D numerical studies of the SSH model have been extended to the 2D Lieb lattice [28], but not to the single orbital square lattice. One measure of the difficulty of analogous higher dimensional studies is the unresolved controversy concerning the optimal bond patterns even with the simplification of completely freezing the lattice distortion. Tang and Hirsch [29] argued that a $\mathbf{q} = (\pi, \pi)$ phonon, polarized along the x-axis (or y-axis), provides the largest energy gain when a displacement δ is introduced to the frozen lattice. Using mean field, they also argued that this (π, π) pattern survives up to a crticial Hubbard coupling, U_c, beyond which the bond order changes to $(\pi, 0)$. These results were challenged by subsequent work [30, 31] where the phonons are allowed to fluctuate, but were taken to be purely classical. The claim here was that the optimal energy was achieved by a superposition of a broad spectrum of lattice momenta, rather than individual values at the borders of the Brillouin zone. Our goal is to clarify this unsettled situation.

Here we present our exact quantum Monte Carlo (QMC) results for the 2D SSH model, with full quantum dynamics of the phonons. We performed the simulations for lattice sizes 8×8, 10×10 and 12×12 with periodic boundary conditions. Larger sizes are not practical

with current algorithms. Our key conclusions are the demonstration, at half filling, of a finite temperature phase transition to an insulating BOW phase, and a quantitative determination of T_c and the associated compressibility gap. Most importantly, we determine the nature of the BOW pattern, thus resolving this long-standing question [29–31]. Furthermore, we present numerical evidence that, in the ground state, the electron-phonon coupling must exceed a finite critical value for BOW to be established, unlike in the Holstein model where the Peierls charge density wave (CDW) phase is present for any finite coupling on a square lattice.

Model and method: We study the two-dimensional "optical" SSH model governed by the Hamiltonian,

$$H = -t \sum_{\langle i,j\rangle,\sigma} (1 - \lambda \hat{X}_{ij})(\hat{c}^\dagger_{i\sigma}\hat{c}_{j\sigma} + \hat{c}^\dagger_{j\sigma}\hat{c}_{i\sigma}) - \mu \sum_{i,\sigma} \hat{n}_{i\sigma} + \sum_{\langle i,j\rangle} \left[\frac{1}{2M}\hat{P}^2_{ij} + \frac{M}{2}\omega_0^2 \hat{X}^2_{ij} \right], \quad (1)$$

where $\hat{c}_{i\sigma}$ ($\hat{c}^\dagger_{i\sigma}$) destroys (creates) an electron of spin σ =↑,↓ on site i and μ is the electron chemical potential. The bond operators $\hat{X}_{ij}$ and $\hat{P}_{ij}$, connecting near neighbor sites $\langle ij\rangle$, are the phonon displacement and momentum, M is an effective mass, ω_0 is an oscillation frequency, and $\lambda = (g/t)\sqrt{2M\omega_0/\hbar}$ is the electron-phonon coupling constant. In the following, we work in units for which $\hbar = t = M = 1$ and fix $\omega_0 = 1$. It was shown in 1D that this model gives the same results as the "acoustic" SSH model [32] where different phonon degrees of freedom are coupled.

For any $g > 0$ at half filling, the 1D model is in the BOW phase [18, 32–35] where the expectation value of the kinetic energy alternates with period π down the chain. To determine the nature of the ground state phase diagram and the finite temperature transition in 2D, we use the exact determinant quantum Monte Carlo (DQMC) method [36–38]. Our main interest is the half filled case ($\mu = 0$); we calculate several quantities needed to characterize the phase diagram: $\langle K_{x(y)}\rangle \equiv \langle \hat{c}^\dagger_{i\sigma}\hat{c}_{i+\hat{x}(\hat{y})\,\sigma}\rangle$, (the average kinetic energies (KE) in the x and y directions) and $\langle X_{x(y)}\rangle$ (the average phonon displacements in the x and y directions) which indicate when x-y symmetry is broken. In addition, the KE bond-bond correlation function, $G_{K_{x(y)}}(r) \equiv \langle K_{x(y)}(i)K_{x(y)}(i+r)\rangle$, is calculated; its Fourier transform (the structure factor, $S_{K_{x(y)}}(k_x, k_y)$) indicates the ordering vector of possible long range BOW. Equilibration of DQMC simulations of electron-phonon Hamiltonians is known to be challenging [38, 39]. Data shown were typically obtained by averaging over ten independent simulations, each using $\mathcal{O}(10^5)$ sweeps of the lattice before making measurements, to ensure thermalization had occurred. DQMC simulations scale as $N^3\beta$, where N is the spatial lattice size and β is the inverse temperature. At large β, $N \sim 10^2$-10^3 are accessible [40, 41]. Because of long equilibration and autocorrelation times in el-ph models, studies are typically limited to the lower end of this range.

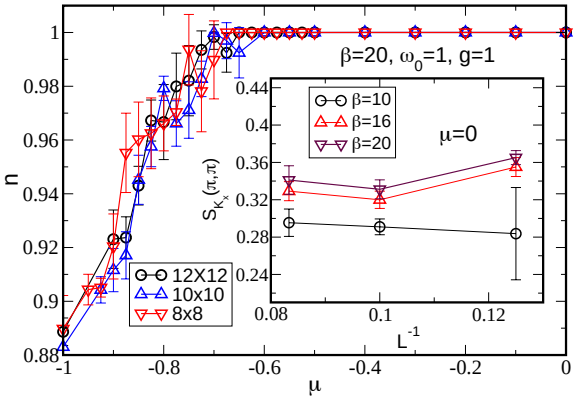

FIG. 1. (Color online) The density, n, versus the chemical potential, μ. The gap is symmetric with respect to $\mu = 0$ due to particle-hole symmetry. The inset shows that long range order, and therefore the gap, achieve their ground state values for these lattice sizes for $\beta \gtrsim 16$.

Results: Figure 1 shows, for $g = 1$, the electron density n versus μ, clearly exhibiting a gapped phase for which the compressibility $\kappa \propto \partial n/\partial\mu = 0$ in the region $-0.7 \lesssim \mu \lesssim +0.7$. The inset shows $S_{K_x}(\pi,\pi)$ for several L and β, establishing finite β effects are negligible for $\beta \geq 16$. The structure factor S provides a more exacting criterion for convergence than a local observable like the density n since it involves long range correlations.

The nature of the gapped phase is exposed by studying $G_{K_{x(y)}}(r)$ (or $G_{X_{x(y)}}(r)$) and the structure factor, $S_{K_{x(y)}}(k_x, k_y)$. In Fig. 2 we plot $S_{K_{x(y)}}(\pi,\pi)$ versus g. At $g \approx 0.75 \pm 0.05$ a quantum phase transition to BOW occurs where $S_{K_x}(\pi,\pi)$ or $S_{K_y}(\pi,\pi)$ acquires nonzero value indicating symmetry breaking. In all cases studied in this paper we measured $S_{K_{x(y)}}(k_x, k_y)$ for all momenta and observe ordering peaks only at (π,π). Starting simulations from several random or ordered phonon initial configurations, Fig. 3, the system only develops checkerboard BOW (for $g > g_c$) either for the x or y bonds but not both simultaneously. This excludes all bond order patterns except the one shown in the inset of Fig. 2 and the three equivalent ones; the broken symmetry is $\mathcal{Z}_4$. To keep figures uncluttered, we show BOW only for x bonds.

When a BOW forms, the x-y symmetry breaking also manifests itself in the $x(y)$ average kinetic energy, $\langle K_{x(y)}\rangle$, and the average phonon displacements $\langle X_{x(y)}\rangle$. Figure 4 shows $\langle K_{x(y)}\rangle$ versus g for systems with $L =$ 8, 10, 12 and three values of the imaginary time step, $d\tau \equiv \beta/L_\tau$ where L_τ is the number of imaginary

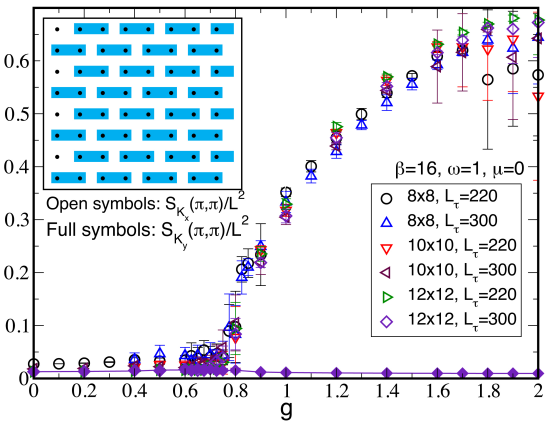

FIG. 2. (Color online) x and y kinetic energy bond-bond structure factors, $S_{K_x}(\pi,\pi)/L^2$ and $S_{K_y}(\pi,\pi)/L^2$, versus g. Long range checkerboard BOW develops for $g \gtrsim 0.75 \pm 0.05$. $S_{K_y}(\pi,\pi)/L^2$ remains very small for all g indicating the order is only in the x bonds.

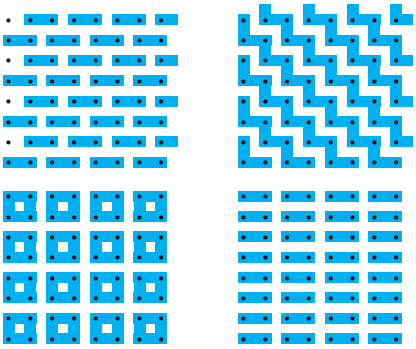

FIG. 3. (Color online) Possible BOW configurations. Top left: (π,π) order of x bonds, top right: (π,π) order of x and y bonds simultaneously, bottom left: (π,π) plaquette order, bottom right: columnar $(\pi,0)$ of x bonds.

time slices in the DQMC. All $d\tau$ values give similar results indicating that $d\tau$ Trotter errors are smaller than the statistical error bars. Figure 4 also shows that for $g \gtrsim 0.75$, the x-y symmetry breaks with the formation of (π,π) BOW in the x direction indicated by larger absolute values for $\langle K_x \rangle$. These conclusions are supported by Fig. 5 which shows the average x and y phonon displacements for the same systems as in Fig. 4. Again, the x and y values bifurcate for $g \gtrsim 0.75$ signalling the x-y symmetry breaking and the formation of BOW. Extrapolating to the thermodynamic limit the values of $g_c(L)$ from Figs. 4 and 5, we find $g_c = 0.67 \pm 0.02$ (inset Fig.5). This relatively large finite value argues that, unlike the one-dimensional SSH model which always

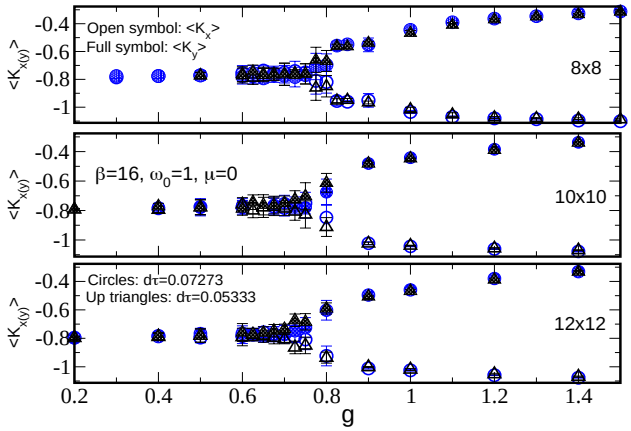

FIG. 4. (Color online) The average kinetic energies in the x and y directions, $\langle K_{x(y)} \rangle$, as functions of g for three system sizes. The bifurcations in the average values indicate the phase transtion breaking the $\mathcal{Z}_4$ symmetry. The inverse temperature $\beta = 16$ ensures that the system is in its ground state for these spatial lattice sizes (see inset to Fig. 1).

displays BOW for any finite g, in two dimensions a finite critical value of g is needed to establish BOW.

Next we study the transition from a disordered phase at high temperature, $T = 1/\beta$, to a BOW as T is lowered. Figure 6 shows $S_{K_x}(\pi,\pi)/L^2$ versus β for system sizes $L = 8, 10, 12$. We see rapid increase in the structure factor as β increases, indicating the establishment of a BOW. The transition shifts to smaller β (higher T) as L increases; the inset shows the bifurcation of $\langle K_{x(y)} \rangle$, and thus the symmetry breaking due to the phase transition. We note the large error bars in $S_{K_x}(\pi,\pi)/L^2$ in the transition region which are caused by outliers which occur in about 10% of the simulations. We also study the finite T transition by examining the specific heat, $C = \partial E/\partial T$, where E is the total energy in the ground state. We show in Fig. 7(a) E/N as a function of T for three sizes, where N is the number of lattice sites. The lines through the symbols are obtained with a third order rational function (Padé) fit. In Fig. 7(b) we show C obtained from the derivative of the Padé fit, the positions of the peaks agree very well with $T_c(L)$ obtained from the inset of Fig. 6. Extrapolating to the thermodynamic limit $T_c(L)$ obtained from Fig. 6 and from the peaks of C yields $T_c = 0.51$ ($\beta_c = 1.96$) and $T_c = 0.52$ ($\beta_c = 1.92$) respectively, as shown in Fig. 7(c).

Conclusions: In the past several years, building on earlier work [37, 38, 42–45], a second generation of QMC has been applied to Hamiltonians coupling phonon modes to the *local electron charge density* [37, 38, 42–49]. In this paper, we report instead QMC simulations of the single orbital square lattice *bond phonon* (SSH) model,

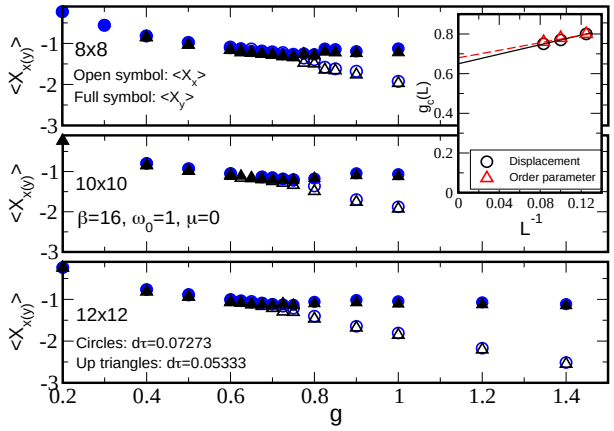

FIG. 5. (Color online) Same as Fig. 4 but for the phonon displacements. The phonon displacement $\langle X_{ij}\rangle$ becomes larger for $j = i + \hat{x}$, than for $j = i + \hat{y}$ at $g > g_c$, indicating a symmetry breaking quantum phase transition. Inset: Circles: extrapolation of the critical coupling from phonon displacement (this figure), $g_c = 0.65$. Triangles: Extrapolation of critical coupling from the order parameter, Fig. 4, $g_c = 0.68$.

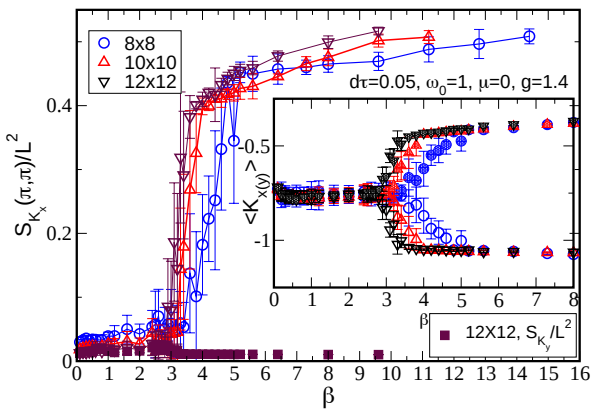

FIG. 6. (Color online) BOW structure factor at (π, π) versus β indicating a thermal phase transition. Inset: The average x (open symbols) and y (full symbols) kinetic energies as functions of β showing a bifurcation consistent with the main panel. Finite size extrapolation gives $\beta_c \approx 1.9$.

including full quantum dynamics, the paradigmatic Hamiltonian describing phonons coupled to electron hopping. Previously, these had been undertaken only in one dimension where they showed the system to be always in the BOW phase for any finite value of the coupling. The "obvious" strong-weak bond alternation pattern in 1D has a multitude of possible generalizations

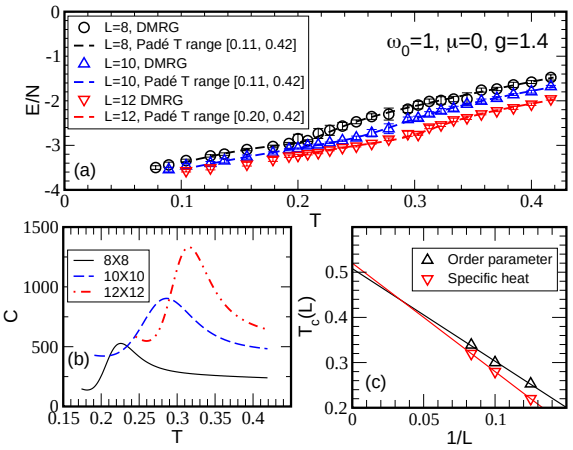

FIG. 7. (Color online) (a) The total energy per site as a function of the temperature, T, at half-filling. The lines are third order rational function (Padé) fits to the data in the corresponding T intervals. (b) The specific heat, C obtained for the derivatives of the Padé fits. (c) Extrapolation to the thremodynamic limit of $T_C(L)$ obtained from the peaks of C and from the order parameter (inset Fig. 6). The specific heat yields $T_C = 0.52$ and the order parameter gives $T_c = 0.51$.

in 2D, including staircase, columnar, staggered, and plaquette arrangements [50], Fig. 3. We have shown that in the ground state, a $\mathbf{q} = (\pi, \pi)$ order is established for x or y bonds (but not both simultaneously), thus resolving a longstanding controversy. We also showed that this bond ordering is accompanied by the opening of a compressibility gap, given by a plateau in $\rho(\mu)$. Furthermore, we have exposed an important qualitative difference between the two- and one-dimensional SSH models: In 2D, a critical value of the coupling, g_c, is necessary to trigger the quantum phase transition from a disordered phase to the BOW, in contradistinction with 1D where the BOW is present for any finite g no matter how small [18, 19, 32–34].

The results presented here focused on the phonon frequency $\omega_0 = 1$. We have confirmed that decreasing ω_0 allows the system to establish BOW at lower but nonzero values of g. For example, for $\omega_0 = 1/2$, BOW sets in at $g \approx 0.5$ for an 8×8 system as opposed to $g \approx 0.7$ for the $\omega_0 = 1$ case on the same 8×8 lattice. This behavior is analogous to the one-dimensional case where the BOW gets stronger at lower values of ω_0 [19, 33] but with the important difference that in one dimension BOW is present for any nonzero value of g [18, 32–35].

The 2D SSH model can be used to understand CDW transition materials such as the transition metal dichalcogenides [51–53], although the accuracy of this modeling is affected by their multi-band character and their complex lattice structures. A more promising experimental connection of the present work is to

bismuthates such as $BaPb_{1-x}Bi_xO_3$ [54–60]. Indeed a study of oxygen breathing modes of a three band SSH model in two dimensions in the context of these materials, has very recently appeared [28]. The bismuthates are, however, not layered. Thus a 3D and 3-band generalization of the present SSH Hamiltonian could provide a fairly close connection to aspects of the bismuthate materials.

In the last year a variant of the 2D SSH model has been realized in acoustic networks [61] and RF circuits [62], allowing the observation of edge states and associated topological invariants [63] within the context of the "plaquette" bond ordering pattern (bottom left, Fig. 3). While this configuration can be engineered artificially, our work shows that the low energy ordering pattern which spontaneously arises from the simplest 2D SSH Hamiltonian, Eq. 1, consists instead of a staggered array of dimers. An interesting area of investigation will be modifications to Eq. 1, for example to the hopping parameters, which might lead to the alternate ordering patterns of Fig. 3, including plaquette arrangements.

Acknowledgments: The work of RTS was supported by the grant DE-SC0014671 funded by the U.S. Department of Energy, Office of Science. We thank B. Cohen-Stead and S. Cui for helpful discussions. D. P. acknowledges support from the Singapore Ministry of Education, Singapore Academic Research Fund Tier-II (Project MOE2016-T2-1-065). The computational work for this article was performed on resources of the National Supercomputing Centre, Singapore (NSCC)[64].

[1] W. P. Su, J. R. Schrieffer, and A. J. Heeger, Phys. Rev. Lett. **42**, 1698 (1979).
[2] H. Keiss, Springer-Verlag Berlin (1992).
[3] T. Ishiguro and K. Yamaji, Springer-Verlag Berlin (1990).
[4] H. Toftlund and O. Simonsen, Inorg. Chem. **23**, 4261 (1984).
[5] M. Hase, I. Terasaki, and K. Uchinokura, Phys. Rev. Lett. **70**, 3651 (1993).
[6] S. Fölling, S. Trotzky, P. Chieinet, M. Feld, R. Saers, A. Widera, T. Müller, and I. Bloch, Nature **448**, 1029 (2007).
[7] J. Sebby-Strabley, M. Anderlini, P. S. Jessen, and J. V. Porto, Phys. Rev. A **73**, 033605 (2006).
[8] M. Atala, M. Aidelsburger, J. Barreiro, D. Abanin, T. Kitagawa, E. Demler, and I. Bloch, Nat. Phys. **9**, 795 (2013).
[9] E. Meier, F. An, and B. Gadway, Nat. Comm. **7**, 13986 (2016).
[10] M. Lohse, C. Schweizer, O. Zilberberg, M. Aidelsburger, and I. Bloch, Nat. Phys. **12**, 350 (2016).
[11] X.-L. Qi and S.-C. Zhang, Rev. Mod. Phys. **83**, 1057 (2011).
[12] A. P. Schnyder, S. Ryu, A. Furusaki, and A. W. W. Ludwig, Phys. Rev. B **78**, 195125 (2008).
[13] J. E. Hirsch and E. Fradkin, Phys. Rev. B **27**, 4302 (1983).
[14] H. Zheng, D. Feinberg, and M. Avignon, Phys. Rev. B **39**, 9405 (1989).
[15] R. H. McKenzie, C. J. Hamer, and D. W. Murray, Phys. Rev. B **53**, 9676 (1996).
[16] M. Weber, F. Parisen Toldin, and M. Hohenadler, Phys. Rev. Research **2**, 023013 (2020).
[17] W. Su, Solid State Commun. **42**, 497 (1982).
[18] W. Barford and R. J. Bursill, Phys. Rev. B **73**, 045106 (2006).
[19] H. Bakrim and C. Bourbonnais, Phys. Rev. B **76**, 195115 (2007).
[20] D. Schmeltzer, R. Zeyher, and W. Hanke, Phys. Rev. B **33**, 5141 (1986).
[21] D. J. J. Marchand, G. De Filippis, V. Cataudella, M. Berciu, N. Nagaosa, N. V. Prokofév, A. S. Mishchenko, and P. C. E. Stamp, Phys. Rev. Lett. **105**, 266605 (2010).
[22] R. T. Clay and R. P. Hardikar, Phys. Rev. Lett. **95**, 096401 (2005).
[23] H. Fehske, G. Hager, and E. Jeckelmann, Europhys. Lett. **84**, 57001 (2008).
[24] J. Greitemann, S. Hesselmann, S. Wessel, F. F. Assaad, and M. Hohenadler, Phys. Rev. B **92**, 245132 (2015).
[25] M. Hohenadler, F. F. Assaad, and H. Fehske, Phys. Rev. Lett. **109**, 116407 (2012).
[26] J. Sous, M. Chakraborty, C. P. J. Adolphs, R. V. Krems, and M. Berciu, Scientific Reports **7** (2017).
[27] J. Sous, M. Chakraborty, R. V. Krems, and M. Berciu, Phys. Rev. Lett. **121**, 247001 (2018).
[28] S. Li and S. Johnston, npj Quantum Materials **5**, 40 (2020).
[29] S. Tang and J. E. Hirsch, Phys. Rev. B **37**, 9546 (1988).
[30] Y. Ono and T. Hamano, J. Phys. Soc. Japan **69**, 1769 (2000).
[31] S. Chiba and Y. Ono, J. Phys. Soc. Japan **73**, 2473 (2004).
[32] M. Weber, F. F. Assaad, and M. Hohenadler, Phys. Rev. B **91**, 245147 (2015).
[33] E. Fradkin and J. E. Hirsch, Phys. Rev. B **27**, 1680 (1983).
[34] P. Sengupta, A. W. Sandvik, and D. K. Campbell, Phys. Rev. B **67**, 245103 (2003).
[35] H. Bakrim and C. Bourbonnais, Phys. Rev. B **91**, 085114 (2015).
[36] R. Blankenbecler, D. J. Scalapino, and R. L. Sugar, Phys. Rev. D **24**, 2278 (1981).
[37] R. T. Scalettar, N. E. Bickers, and D. J. Scalapino, Phys. Rev. B **40**, 197 (1989).
[38] R. M. Noack, D. J. Scalapino, and R. T. Scalettar, Phys. Rev. Lett. **66**, 778 (1991).
[39] G. G. Batrouni and R. T. Scalettar, Phys. Rev. B **99**, 035114 (2019).
[40] C. N. Varney, C.-R. Lee, Z. J. Bai, S. Chiesa, M. Jarrell, and R. T. Scalettar, Phys. Rev. B **80**, 075116 (2009).
[41] G. G. Batrouni and R. T. Scalettar, Journal of Physics: Conference Series **1290**, 012004 (2019).
[42] M. Vekic, R. M. Noack, and S. R. White, Phys. Rev. B **46**, 271 (1992).
[43] P. Niyaz, J. E. Gubernatis, R. T. Scalettar, and C. Y. Fong, Phys. Rev. B **48**, 16011 (1993).
[44] F. Marsiglio, Phys. Rev. B **42**, 2416 (1990).
[45] M. Hohenadler, H. G. Evertz, and W. von der Linden,

Phys. Rev. B **69**, 024301 (2004).
[46] M. Weber and M. Hohenadler, Phys. Rev. B **98**, 085405 (2018).
[47] C. Chen, X. Y. Xu, Z. Y. Meng, and M. Hohenadler, Phys. Rev. Lett. **122**, 077601 (2019).
[48] Y.-X. Zhang, W.-T. Chiu, N. C. Costa, G. G. Batrouni, and R. T. Scalettar, Phys. Rev. Lett. **122**, 077602 (2019).
[49] B. Cohen-Stead, N. C. Costa, E. Khatami, and R. T. Scalettar, Phys. Rev. B **100**, 045125 (2019).
[50] J. E. Hirsch and S. Tang, Phys. Rev. Lett. **62**, 591 (1989).
[51] R. L. Withers and J. A. Wilson, Journal of Physics C: Solid State Physics **19**, 4809 (1986).
[52] A. H. Castro Neto, Phys. Rev. Lett. **86**, 4382 (2001).
[53] K. Rossnagel, J. Phys.: Condens. Matter **23**, 213001 (2011).
[54] A. W. Sleight, J. L. Gillson, and P. E. Bierstedt, Solid State Communications **17**, 27 (1975).
[55] A. W. Sleight, J. L. Gillson, and P. E. Bierstedt, Solid State Comm. **88**, 841 (1993).
[56] S. Uchida, K. Kitazawa, and S. Tanaka, Phase Trans. **8**, 95 (1987).
[57] L. F. Mattheiss and D. R. Hamann, Phys. Rev. Lett. **60**, 2681 (1988).
[58] L. F. Mattheiss, E. M. Gyorgy, and D. W. Johnson, Phys. Rev. B **37**, 3745 (1988).
[59] R. J. Cava, B. Batlogg, J. J. Krajewski, R. Farrow, L. W. R. Jr, A. E. White, K. Short, W. F. Peck, and T. Kometani, Nature **332**, 814 (1988).
[60] R. J. Cava, B. Batlogg, G. P. Espinoza, A. P. Ramirez, J. J. Kajewski, W. P. Jr., L. W. R. Jr., and A. S. Cooper, Nature **339**, L291 (1989).
[61] L.-Y. Zheng, V. Achilleos, O. Richoux, G. Theocharis, and V. Pagneux, Phys. Rev. Applied **12**, 034014 (2019).
[62] S. Liu, W. Gao, Q. Zhang, S. Ma, L. Zhang, C. Liu, Y. J. Xiang, T. J. Cui, and S. Zhang, Research , 8609875 (2019).
[63] D. Obana, F. Liu, and K. Wakabayashi, Phys. Rev. B **100**, 075437 (2019).
[64] https://www.nscc.sg .